Published in final edited form as:

Appl Radiat Isot. 2017 September ; 127: 52–60. doi:10.1016/j.apradiso.2017.05.006.

Automated cassette-based production of high specific activity [$^{203/212}$pb] peptide-based theranostic radiopharmaceuticals for image-guided radionuclide therapy for cancer

Mengshi Li[a,1], **Xiuli Zhang**[b], **Thomas P. Quinn**[b], **Dongyoul Lee**[a], **Dijie Liu**[c], **Falk Kunkel**[d], **Brian E. Zimmerman**[e], **Daniel McAlister**[f], **Keith Olewein**[g], **Yusuf Menda**[h], **Saed Mirzadeh**[i], **Roy Copping**[i], **Frances L. Johnson**[j,k], and **Michael K. Schultz**[a,c,h,j,l,m,*]

[a]Interdisciplinary Graduate Program in Human Toxicology, University of Iowa, Iowa City, IA, USA

[b]Department of Biochemistry, University of Missouri, Columbia, MO USA

[c]Stead Family Department of Pediatrics, University of Iowa, Iowa City, IA, USA

[d]Eckert & Ziegler Radiopharma GmbH, Berlin, Germany

[e]National Institute of Standards and Technology, Gaithersburg, MD, USA

[f]Eichrom Technologies, LLC, Lisle, IL, USA

[g]Lantheus Medical Imaging North Billerica, MA, USA

[h]Department of Radiology, The University of Iowa, Iowa City, IA, USA

[i]Oak Ridge National Laboratory, The US Department of Energy, Oak Ridge, TN, USA

[j]Viewpoint Molecular Targeting, LLC, Coralville, IA, USA

[k]Department of Internal Medicine, Carver College of Medicine, University of Iowa, Iowa City, IA, USA

[l]Department of Radiation Oncology (Free Radical and Radiation Biology Program), Carver College of Medicine, University of Iowa, Iowa City, IA, USA

[m]Department of Chemistry, University of Iowa, Iowa City, IA, USA

Abstract

A method for preparation of Pb-212 and Pb-203 labeled chelator-modified peptide-based radiopharmaceuticals for cancer imaging and radionuclide therapy has been developed and adapted for automated clinical production. Pre-concentration and isolation of radioactive Pb2+ from interfering metals in dilute hydrochloric acid was optimized using a commercially-available Pb-specific chromatography resin packed in disposable plastic columns. The pre-concentrated radioactive Pb2+ is eluted in NaOAc buffer directly to the reaction vessel containing chelator-

*Correspondence to: Departments of Radiology, Radiation Oncology, Chemistry, and Pediatrics, The University of Iowa, ML B180 FRRBP, 500 Newton Road, Iowa City, IA 52240, USA. mengshi-li@uiowa.edu (M. Li), michael-schultz@uiowa.edu (M.K. Schultz).

[1]First Author: Mengshi Li MS. Graduate Researcher (PhD). Interdisciplinary Program in Human Toxicology, ML B180 FRRB, 500 N Road, Iowa City, IA 52240, USA.

Appendix A. Supplementary material

Supplementary data associated with this article can be found in the online version at http://dx.doi.Org/10.1016/j.apradiso.2017.05.006.

modified peptides. Radiolabeling was found to proceed efficiently at 85 °C (45 min; pH 5.5). The specific activity of radiolabeled conjugates was optimized by separation of radiolabeled conjugates from unlabeled peptide *via* HPLC. Preservation of bioactivity was confirmed by *in vivo* biodistribution of Pb-203 and Pb-212 labeled peptides in melanoma-tumor-bearing mice. The approach has been found to be robustly adaptable to automation and a cassette-based fluid-handling system (Modular Lab Pharm Tracer) has been customized for clinical radiopharmaceutical production. Our findings demonstrate that the Pb-203/Pb-212 combination is a promising elementally-matched radionuclide pair for image-guided radionuclide therapy for melanoma, neuroendocrine tumors, and potentially other cancers.

Keywords

Radionuclides; Pb-203; Pb-212; Alpha particle therapy; Peptides; Radiopharmaceuticals

1. Introduction

Receptor-targeted image-guided radionuclide therapy is increasingly recognized as a promising approach to treating cancer. (Bartlett, 2016; Hardiansyah et al., 2016; Iagaru et al., 2016; Jin et al., 2016; Kratochwil et al., 2016a; Kratochwil et al., 2016b; Kwekkeboom and Krenning, 2016; Li et al., 2016; Lo Russo et al., 2016; Nonnekens et al., 2016; Norain and Dadachova, 2016; Otte, 2016; Takahashi et al., 2016; Weber and Morris, 2016; Werner et al., 2016; Zukotynski et al., 2016) In particular, the potential for clinical translation of receptor-targeted alpha-particle (α-) therapy is receiving considerable attention; and several recent works have highlighted the potential advantages of α-therapy.(Bartlett, 2016; Iagaru et al., 2016; Kratochwil et al., 2016a; Kratochwil et al., 2016b; Kwekkeboom and Krenning, 2016) Alpha emitters are emerging as an attractive alternative (to α-emitters) due to higher linear-energy transfer (LET) (100 keV/μm) and resultant-significant increase in the intensity of ionizations (primary and secondary) along the relatively short path length that α-particles travel in tissue (compared to β-particles).(Wild et al., 2011; Iagaru et al., 2016; Kratochwil et al., 2016a; Kratochwil et al., 2016b; Otte, 2016; Takahashi et al., 2016; Zukotynski et al., 2016) These properties have been shown to result in an increased incidence of double-strand DNA breaks and improved-localized cancer-cell damage that convey the potential for more effective tumor-cell-specific killing with less damage to adjacent-normal cells (*i.e.*, improved relative biological effectiveness; RBE). (Sgouros, 2008; Sgouros et al., 2010; Sgouros et al., 2011; Hobbs et al., 2014; Macklis et al., 1988; Humm and Chin, 1993; Hauck et al., 1998; McDevitt et al., 1998; Behr et al., 1999; Behr et al., 2001; Jurcic et al., 2002; Akabani et al., 2003; Miao et al., 2005; Zalutsky, 2006; Sgouros, 2008; Sgouros and Song, 2008; Sgouros et al., 2010; Sgouros et al., 2011; Kim and Brechbiel, 2012; Elgqvist et al., 2014; Hobbs et al., 2014; Kratochwil et al., 2014; Wadas et al., 2014; Kratochwil et al., 2016a; Kratochwil et al., 2016b) For example, recent studies in patients with advanced-stage castration-resistant metastatic prostate cancer provide compelling evidence that α-therapy (using [^{225}Ac]PSMA617) has the potential to deliver a significantly more potent anti-cancer effect compared with β-therapy (using [^{177}Lu]PSMA617).(Kratochwil et al., 2016a; Kratochwil et al., 2016b) Numerous other studies demonstrate the potential of α-emitters for cancer therapy using radionuclides ^{225}Ac, ^{212}Bi, ^{213}Bi, and ^{211} At.(Macklis et al., 1988;

Humm and Chin, 1993; Hauck et al., 1998; McDevitt et al., 1998; Behr et al., 1999; Behr et al., 2001; Jurcic et al., 2002; Akabani et al., 2003; Miao et al., 2005; Zalutsky, 2006; Sgouros, 2008; Sgouros and Song, 2008; Sgouros et al., 2010; Sgouros et al., 2011; Wild et al., 2011; Kim and Brechbiel, 2012; Elgqvist et al., 2014; Hobbs et al., 2014; Kratochwil et al., 2014; Wadas et al., 2014; Kratochwil et al., 2016a; Kratochwil et al., 2016b) Generator-produced ^{212}Pb (which decays to alpha emitters ^{212}Bi and ^{212}Po) is a particularly promising radionuclide for receptor-targeted α-particle therapy for metastatic melanoma and neuroendocrine tumors, and other cancers (Fig. 1).(Miao et al., 2005; Miao et al., 2008; Miao and Quinn, 2008; Martin et al., 2013; Norain and Dadachova, 2016).

Due to the nature of α-decay, direct non-invasive molecular imaging of the *in vivo* pharmacokinetics and biodistribution *via* α-emissions is not possible. However, an understanding of the pharmacokinetics and biodistribution of receptor-targeted candidate ligands is desirable for developing appropriate dosimetry and treatment plans in advance of the radionuclide therapy. In previous studies, non-invasive imaging of the extent of disease has been conducted using [^{68}Ga]DOTATOC and [^{68}Ga]PSMA617 in advance of therapy *via* [^{213}Bi]DOTATOC and[^{225}Ac] PSMA617 respectively. While these studies reflect the potential of the theranostic approach, using isotopes of different elements in the imaging and therapeutic procedures introduces some ambiguity in the effectiveness of the imaging agent to predict the *in vivo* pharmacodynamics of the radiotherapeutic ligands. For example, recent comparisons of tumor and normal organ uptake of [^{68}Ga]DOTATOC *vs* [^{90}Y]DOTATOC revealed small, but measurable, differences in normal organ accumulation between the agents that may be attributable to differences in Ga and Y chemistry.(Fani and Maecke 2012).

In our proposed application, the gamma(γ)-emitting radionuclide ^{203}Pb is being explored as the imaging surrogate for the therapeutic nuclide ^{212}Pb.(Miao et al., 2005; Miao et al., 2008; Miao and Quinn, 2008; Norain and Dadachova, 2016) The use of an isotope of the same element adds confidence to predictions that images collected are an appropriate representation of the expected pharmacokinetics/biodistribution of the therapeutic ligand. Within this context, our laboratories are pursuing ^{203}Pb (half life $t_{1/2}$ =52 h; gamma-ray intensity 81%; 279 keV) and ^{212}Pb ($t_{1/2}$ = 11 h; 100% β decay to α-emitters ^{212}Bi and ^{212}Po) as elementally-matched radionuclides. Importantly, the decay of ^{212}Pb includes the emission of a gamma ray with an energy (238 keV) that has the potential to enable direct imaging *via* SPECT of [^{212}Pb]-labeled peptides. While this property of ^{212}Pb nuclear decay may present opportunities for direct imaging of the biodistribution of [^{212}Pb]-labeled peptides in the future, the use of ^{203}Pb enables a non-invasive ^{203}Pb SPECT (or SPECT/CT) image to be collected in advance of ^{212}Pb receptor-directed radiotherapy, with minimal risk of an adverse event. Thus, the potential value of this approach also conveys an improved patient selection for inclusion in clinical trials and a higher likelihood for approvals of ^{212}Pb labeled therapies. In addition, ^{203}Pb is conveniently produced by commercial cyclotron (see Supplemental Information), and ^{212}Pb is obtained (for radiopharmaceutical purposes) *via* a ^{224}Ra/^{212}Pb generator (Fig. 1; and Supplemental Information). Advanced studies to develop a more detailed understanding of the potential for migration of ^{212}Pb decay-product progeny (*i.e.*, ^{212}Bi; ^{212}Po; Fig. 1) away from the decay of ^{212}Pb *in vivo* are an important aspect of current research in our laboratories and beyond the scope of the current article.

Here, we present the development of an automated cassette-based approach to $^{203/212}$pb radiolabeling and purification of chelator-modified peptides that can be easily integrated into routine clinical production (Fig. 2). Extraction chromatography was used to facilitate pre-concentration of both cyclotron-produced ^{203}Pb and generator produced ^{212}Pb. An HPLC approach for isolation of final-product radiopharmaceutical was optimized to enable automation of ^{203}Pb and ^{212}Pb radiolabeled peptides from unlabeled precursors and achievement of near theoretical specific activity (MBq nmol^{-1}). An examination of the analogous *in vitro* and *in vivo* biochemical behavior of the ^{203}Pb and ^{212}Pb labeled peptides (in melanoma-tumor bearing mice) is presented as evidence that the bioactivity of the compounds (following automated production) is preserved. These studies further corroborate previous preclinical reports supporting the use of ^{203}Pb as a surrogate-imaging radionuclide for use in advance of ^{212}Pb therapy. Results demonstrate the feasibility of automated preparation of ^{203}Pb and ^{212}Pb radiopharmaceuticals for clinical use and provide guidance for further refinements potentially necessary to adapt the approach for other radiopharmaceutical platforms (*e.g.*, antibodies; aptamers; and small molecules). The sum of the findings and observations presented here support the idea that ^{203}Pb and ^{212}Pb represent a promising elementally-matched radionuclide pair that can be applied clinically for image-guided radionuclide therapy for melanoma; neuroendocrine tumors; and other cancers as well.

2. Materials and methods

2.1. Chemicals and Reagents

Hydrochloric acid (Trace Metal Grade) was purchased from Fisher Chemical. ARISTAR® ULTRA metal-free water was obtained from VMR international (Radnor, PA). All other chemical reagents and materials were the highest grade available from Sigma Aldrich and used (as received) without further purification (unless otherwise described). DOTATOC (Fig. 2B) was kindly provided by M. Sue O'Dorisio MD PhD (Stead Family Department of Pediatrics; The University of Iowa (Iowa City, IA USA); and DOTA-PEG4-VMT-MCR1 (Fig. 2C) was purchased commercially (Peptides International Inc.; Louisville, KY USA). Pb-resin™ (100–150 μm) is available commercially from Eichrom Technologies LLC (Lisle, IL USA). The ^{224}Ra/^{212}Pb generators used for these studies were purchased through the Isotopes Program; US Department of Energy; Oak Ridge National Laboratory (see Supplemental Information; ORNL; Oak Ridge, TN USA). ^{203}Pb was provided by Lantheus Medical Imaging (see Supplemental Information; North Billerica, MA USA) in approximately 1 mL of 0.5 M HCl.

2.2. Safety

^{212}Pb decays by β-particle emission to ^{212}Bi, which decays by mixed α-/β-particle emissions to ^{208}Tl, ^{212}Po, and finally to stable ^{208}Pb (Fig. 1). Appropriate precautions must be put in place to prevent exposure of personnel to these radionuclides. Experiments must be conducted in a Pb-shielded environment that is sufficient to reduce potential exposure to γ-radiation emitting *via* decay of ^{208}Tl (2.6 MeV). Utilization of completely enclosed fluid handling systems and work in HEPA filtered fume hoods may be appropriate to mitigate the risk of inhalation or exposure. For our studies, exposures (as radioactivity levels were

increased) were minimized by use of the automated-enclosed fluid-handling system in a Pb-shielded (4–6″) environment. The $^{224}Ra/^{212}Pb$ generator is equipped with an inlet and outlet that enable a complete closed loop system connected directly to the sterile-GMP manufactured cassette (Eckert Zeigler, Berlin Germany). Similar radiation safety plans must be in place for use of ^{203}Pb.

2.3. $^{203}Pb/^{212}Pb$ Preconcentration and Analysis

2.3.1. Pb^{2+} and metal breakthrough—

^{203}Pb for the current studies was produced by Lantheus Medical Imaging *via* cyclotron irradiation of natural Tl (^{nat}Tl) targets with 26.5 MeV protons. After suitable decay time for the ^{201}Pb byproduct, ^{203}Pb was separated from the Tl target using routine protocols (Supplemental material). Pb-resin, comprising an 18-Crown-6 ether derivative adsorbed to semi-porous beads (100–150 μm particle size; Eichrom Technologies, Lisle, IL USA) was slurried in 0.5–2 M HCl to prepare a 10 mg/mL stock suspension. The appropriate amount of resin was then packed into solid-phase-extraction (SPE) cartridges. Packed columns were capped with frits (20 μm pore size) and rinsed with HCl to remove suspended residues. A breakthrough study was performed to understand the retention of Pb from 2 M HCl carrier solution and the separation of Pb from key metal ion impurities (Cu, Fe, Tl).

2.3.2. $^{203/212}pb^{2+}$ pre-concentration and elution—

For the manual pre-concentration of ^{203}Pb, 370-555MBq $^{203}Pb^{2+}$ (in 2 M HCl) was transferred to the Pb-resin cartridge, which retains Pb, while other metallic potential interferences pass through the SPE cartridge to waste with the HCl carrier. $^{203}pb^{2+}$ was then stripped from the cartridge using 2 mL 0.5 M NaOAc buffer (pH = 6), which was used directly for the following radiolabeling reaction with the test DOTA peptides. Similarly for manual pre-concentration of ^{212}Pb, ~140MBq of ^{212}Pb solution (4–6 mL of 2 M HCl) was eluted slowly (—2 mL per minute) from the $^{224}Ra/^{212}Pb$ generator, collected, and divided into 4 equal aliquots. One aliquot was used as self-reference and others (n = 3) were pre-concentrated in the same manner as described for ^{203}Pb. Both ^{212}Pb and ^{203}Pb activity and recovery from Pb-resin were measured by Capintec CRC25R dose calibrator according to the manufacturer's instructions (dial setting 344 for ^{203}Pb; and dial setting 158 for ^{212}Pb). Both $^{212}pb^{2+}$ reference and eluates were measured and compared with reference after 6 h re-equilibration between ^{212}Pb and ^{212}Bi. Sodium iodide gamma spectrometry was used to determine the radionuclide contents before and after purification by monitoring ^{212}Pb at 238 keV and ^{212}Bi at 583 keV and 860 keV. Other metallic contaminants were determined by mass spectrometry at the University of Iowa State Hygienic Laboratory (Coralville, IA) by routine metal analysis methods following decay of radioactivity.

2.3.3. Radiosynthesis of [$^{203}Pb/^{212}Pb$]DOTATOC and of [$^{203}Pb/^{212}Pb$] DOTA-PEG4-VMT-MCR1—

Following the pre-concentration step, $^{203/212}pb^{2+}$ was eluted from the Pb-resin columns with pH = 6 NaOAc buffer for the radiolabeling reaction. The reaction vessel was pre-loaded with 50 μg peptide suspended in 290 μL pH = 4 NaOAc buffer to adjust the final pH to 5.3–5.5; and the reaction vessel was heated at 85 °C for 45 min (conditions optimized previously).(Baidoo, Milenic et al., 2013) Radiolabeling efficiency (the percentage of incorporated radionuclide from radiolabeling reaction) and radiochemical

purity (the fraction of the stated isotope present in the stated chemical form) (Grieken and de Bruin, 2009) [^{203}Pb/^{212}Pb]Peptides was analyzed by radio-ITLC and radio-HPLC method (Supplemental material). Separation/isolation of radiolabeled DOTA-conjugates from unlabeled peptide *via* HPLC was also investigated (Supplemental material).

2.3.4. Animal pharmacokinetics study—To further evaluate the concept of using [^{203}Pb]-labeled peptide as an imaging surrogate for [^{212}Pb]-labeled peptide therapy, we performed *in vivo* pharmacokinetics studies in B16/F1 murine melanoma tumor-bearing C57/BL6 mice using the test compound DOTA-PEG4-VMT-MCR1, which targets melanocortin subtype1 receptor (MCR1; highly expressed in B16 cells). Mice were subcutaneously inoculated with 10^6 B16/F1 murine melanoma cells in the left shoulder. When tumor size reached about 0.2 g, 3.7–7.4×10^{-3}MBq of HPLC-purified [^{203}Pb]DOTA-PEG4-VMT-MCR1 was injected into each animal *via* the tail vein. In a separate study, [^{212}Pb]DOTA-PEG4-VMT-MCR1 was injected *via* the tail vein in the same type of tumor-bearing xenograft mouse model. The mice were euthanized at 1 and 3 h (n = 3 at each time point) post-injection of radiopharmaceutical. Tumors and organs of interest were harvested, weighed, and measured by NaI gamma spectroscopy using the Maestro multi-channel analyzer (ORTEC, Oak Ridge TN). The results were expressed as percent injected dose per gram (%ID/g) ± SD.

2.3.5. Automated production of [$^{203/212}$Pb]DOTA-pepdde—Adoption of the radiochemical methods presented above for routine clinical application requires automation to facilitate consistent production and to minimize personnel dose considerations. Within this context, fluid handling for pre-concentration of Pb isotopes, radiolabeling of peptide precursors, and separation/isolation/filter sterilization of radiolabeled peptide from unlabeled precursor were integrated into a fully automated cassette-based fluid handling system (Modular Lab Pharm Tracer system (MLPT; Eckert Ziegler, Berlin Germany). The MLPT has been used for several years for the production of [^{68}Ga] DOTATOC and [^{90}Y]DOTATOC and other clinically-relevant radiopharmaceuticals in the PET Center and Nuclear Medicine production facilities at the University of Iowa; and elsewhere. To further evaluate the radiolabeling method for [$^{203/212}$Pb]radiopharmaceutical production, the MLPT cassette system and software were modified to integrate the pre-concentration of $^{203/212}$pb; radiolabeling of precursor DOTA-PEG4-VMT-MCR1 peptide, and final HPLC isolation of $^{203/212}$pb peptide. The $^{203/212}$pb^{2+} pre-concentration; elution; radiolabeling; and HPLC isolation of the $^{203/212}$Pb-final product were carried out as described above. The product from radio-HPLC collection was finally reformulated in ethanol/saline solution and purified *via* Strata-X polymeric reverse cartridge (Phenomenex, Torrance, CA), as we have described previously. (Martin, Sue O'Dorisio et al., 2013) Final radiolabeling efficiency and radiochemical purity of the $^{203/212}$pb labeled peptides were measured as described above.

3. Results

3.1. ^{203}Pb/^{212}Pb pre-concentration and purification

Pre-concentration of ^{203}Pb^{2+} and ^{212}pb^{2+} from solutions of 0.5–2 M HCl was achieved using a Pb-specific extraction chromatography resin. It was found (using a 50 mg resin bed)

that virtually no breakthrough was observed within 5 mL of 2 M HCl and majority of metallic contaminants were removed within 2 resin-bed volumes (~0.1 mL) (Fig. S1). Greater than 95% recovery was achieved for both the $^{203}pb^{2+}$ and $^{212}pb^{2+}$ at the elution step (*i.e.*, following pre-concentration). After elution with pH = 6 NaOAc buffer, $^{203}pb^{2+}$ and $^{212}pb^{2+}$ were used directly for radiolabeling. For ^{212}Pb radiolabeling applications, the Pb-resin efficiently retained $^{212}pb^{2+}$ and removed $^{212}Bi^{2+}$ at the preconcentration step, simplifying the radiochemical make-up of the resulting radiopharmaceutical at the radiolabeling step (Fig. 3). Metal mass spectroscopy results showed that the level of Fe (an interference for the radiolabeling step) in the ^{203}Pb solution was reduced from 46.2 μg to less than 1 μg. All other metal impurities were similarly reduced to levels that did not interfere with the radiolabeling step, while retaining high Pb recovery. (Supplemental Fig. S1; Table S1).

3.2. [^{203}Pb]DOTA-peptide radiolabeling

Following the pre-concentration step, in which the Pb isotopes are isolated from potential metallic interferences using Pb-resin, the Pb is eluted directly into the radiolabeling reaction vessel containing peptide. Two test peptides (DOTATOC and DOTA-PEG4-VMT-MCR1) were used to evaluate the radiolabeling step for manual and automated methods presented here. As determined by HPLC, the radiochemical purity of [^{203}Pb]DOTA-PEG4-VMT-MCR1 (Retention time 17.6 min) was > 98%; with negligible unbound $^{203}pb^{2+}$ present (Fig. 4A). In a separate experiment (Fig. 4B), similar radiochemical purity was observed with [^{203}Pb]DOTATOC (retention time 18.2 min). By co-injecting [^{203}Pb] DOTA-peptide with 10 μg bulk unlabeled peptide, the separation could be monitored by both UV at 280 nm and by radiometric detection (Fig. 4 A&B inset). These data identified sufficient retention time differential between labeled and unlabeled peptide (1.5–2 min) to allow for efficient separation of the labeled from unlabeled peptide; and thus, isolation of high specific activity radiopharmaceutical ([$^{203/212}$Pb] DOTATOC and [$^{203/212}$Pb]DOTA-PEG4-VMT-MCR1) from unlabeled precursor peptide.

3.3. [^{212}Pb]peptide radiolabeling

Similar methodology was applied to [^{212}Pb]peptide radiolabeling. Both [^{212}Pb]DOTA-PEG4-VMT-MCR1 and [^{212}Pb]DOTATOC retention times matched with their ^{203}Pb variants (Fig. 5), providing evidence of the similarity in physico-chemical properties of peptides labeled with [^{203}Pb] and [^{212}Pb]. On the other hand, notable differences were observed in the retention time of [^{212}Pb]DOTATOC compared to [^{212}Bi]DOTATOC (Fig. 5B). The contents of these peaks were isolated and measured by NaI gamma spectroscopy to confirm their radionuclide composition, demonstrating the potential to isolate pure [^{212}Pb]DOTATOC from unlabeled precursor and peptide labeled with decay product radionuclide ^{212}Bi (Fig. 5D). To verify the radiolabeling efficiency of ^{212}Pb labeled peptides, iTLC analysis was applied (Fig. 5C). After overnight decay and re-equilibration, no observable free $^{212}pb^{2+}$ was found at solvent front (Rf=1), whereas > 98% [^{212}Pb]peptide was observed at origin (Rf=0).

3.4. Animal pharmacokinetic/biodistribution study

To confirm that the compounds retained bioactivity and to examine the similarity in the *in vivo* behavior of the [^{203}Pb/^{212}Pb]-labeled counterparts, pharmacokinetic/biodistribution studies were performed with [^{203}Pb]DOTA-PEG4-VMT-MCR1 and [^{212}Pb]DOTA-PEG4-VMT-MCR1 in B16F1 murine melanoma tumor-bearing mice. Both [^{203}Pb/^{212}Pb]DOTA-PEG4-VMT-MCR1 exhibited similar accumulation and retention in the melanoma tumors and kidney, a major dose-limiting organ of peptide-receptor image-guided radionuclide therapy for cancer (Fig. 6 and Table 1). Rapid tumor uptake of [$^{203/212}$pb] DOTA-PEG4-VMT-MCR1 was observed (5.2 ± 0.8% *vs.* 5.5 ± 0.2% at 1 h and 5.2 ± 0.7% *vs.* 4.1 ± 0.5% at 3 h). Similar results were obtained in kidney, [^{203}Pb]DOTA-PEG4-VMT-MCR1 has 17.2 ± 1.3% ID/g at 1 h and 9.9 ± 1.4%ID/g at 3 h, whereas [^{212}Pb]DOTA-PEG4-VMT-MCR1 was 14.8 ± 1.3%ID/g at 1 h and 10.7 ± 0.2%ID/g at 3 h, demonstrating significant kidney clearance in three hours post injection of the radiopharmaceutical. Both ligands had rapid total clearance and low residues in blood and other major tissues after 1 h post-injection.

3.5. Automated radiolabeling method

To explore the potential of this radiolabeling method for routine radiopharmaceutical production in the clinical setting, the manual preparation was adapted to an automated system for labeling of DOTA-PEG4-VMT-MCR1 on the Modular-Lab PharmTracer cassette-based automated fluid handling module (Eckert & Ziegler) (Fig. 6B). The MLPT system allows for adaptation of customized-GMP-grade cassette-based fluid handling for routine clinical production. The complete process for pre-concentration of ^{203}Pb and ^{212}Pb, elution and radiolabeling, and HPLC final purification steps was integrated into the cassette-based hardware system and the system software was modified to account for the modifications for fluid handling (liquid volumes, flow rates, reaction temperatures, hold times, *etc.*). Achievable radiochemical purity using the automated system was consistently greater than 95% (Fig. 6A, retention time = 20 min) after the radiolabeling step; and nearly 100% following the HPLC isolation step. In-line HPLC allowed isolation and collection of [^{212}Pb]DOTA-PEG4-VMT-MCR1 from decay daughters and unlabeled peptide (Fig. 6A, retention time = 20 min). Overall recovery of ^{203}Pb-conjugate was 72% after radio-HPLC collection and final reformulation on Strata-X reverse phase cartridge. A pH of 5 was consistently observed for all final product solutions. (Fig. 7).

4. Discussion

4.1. $^{203Pb/212}$pb^{2+} preconcentration and purification

A method for pre-concentration and purification ^{203}Pb and ^{212}Pb for clinical nuclear medicine applications has been developed and adapted for automated clinical production. The approach employs a commercially-available extraction chromatography resin based on an 18-Crown-6 crown ether adsorbed on a semi-porous substrate and packed in a common disposable SPE cartridge. The pre-concentration step enables a straightforward adaptation of the approach for pre-concentration of ^{203}pb^{2+} produced *via* medical cyclotron; and generator produced ^{212}Pb^{2+}. The method effectively removed potential interfering metal ion impurities, including Fe, Cu, and Tl from cyclotron produced ^{203}Pb and daughter radionuclides arising from the decay of parent radionuclide ^{224}Ra from ^{224}Ra/^{212}Pb

generators. Inclusion of the pre-concentration step is advantageous in that the approach can easily be adapted for radiolabeling of a variety of chelator-modified ligands under a variety of pH and buffer conditions. The approach also removes large volumes of eluent associated with generator elutions; allowing for exchange of acidic carrier solution and elution of the purified $^{203/212}$Pb in the smallest possible volume of NaOAc buffer. Thus, the approach can be modified easily for reacting with a wide selection of precursors for the radiolabeling step. The inclusion of this step overcomes potential drawbacks that limit traditional methods for this purpose. Examples of time-consuming intermediate steps eliminated by preconcentration include evaporation of elution solutions and solvents; and the use of organic solvents, which requires additional efforts to remove these solvents and potentially further QC testing as part of release criteria.(Baidoo et al., 2013; Horwitz et al., 1992; Horwitz et al., 1994) While traditional ion exchange methods often lack selectivity for Pb^{2+} over important metal ion impurities from highly acidic carrier solutions, the 4′,4″(5″)-Di-*tert*-butyldicyclohexano-18-crown-6, is supremely selective for Pb^{2+} under the conditions used for pre-concentration here. (Horwitz et al., 1992; Horwitz et al., 1994) Thus, the approach is advantageous in comparison to previous direct labeling methods introduced previously. It was further shown that the extraction chromatography approach could be efficiently integrated into an automated fluid handling system adapted for routine clinical production of both ^{203}Pb and ^{212}Pb chelator-modified radiopharmaceuticals. Results of radiolabeling experiments using three different DOTA-peptide conjugates typically produced radiochemical purity greater than 98% and nearly 100% radiochemical purity when combined with the automated HPLC final purification.

For ^{212}Pb radiolabeled compounds, both radio-HPLC and iTLC were used for quality control of the final product. Initial radio-HPLC indicated a small fraction of unbound radionuclide and another major radiochemical peak in [^{212}Pb]DOTATOC chromatograms. The material in these peaks was collected and measured by gamma spectrometry and found to be attributed to ^{208}Tl. These results indicate that ^{212}Pb has stable chelation with DOTA and decoupled $^{212}Bi^{3+}$ was generated from the recoil energy of ^{212}Pb decay. The radiolabeling efficiency was further confirmed by iTLC imaging, where the samples were allowed sufficient decay time for complete decay of free ^{212}Bi and equilibrium between ^{212}Pb/^{212}Bi. Because the recoil energy from ^{212}Pb decay constantly generates free $^{212}Bi^{3+}$, these results point to the need for studies designed to more precisely understand the potential for migration of ^{212}Pb decay product radionuclides away from the ^{212}Pb labeled peptides in the *in vivo* setting. In addition, these results point to the need to develop radioligands and delivery formulations that promote rapid tumor uptake; fast ligand endocytosis; prolonged tumor retention; and rapid overall clearance.

4.2. Final HPLC isolation of $^{203/212}$Pb labeled peptides

Radiolabeled peptides were successfully isolated from unlabeled peptide using a radio-HPLC procedure After chelation, the negative charges on the carboxyl acid arms of DOTA are partially neutralized by Pb^{2+}, enhancing the overall lipophilicity of the Pb labeled compound. Therefore, the radiolabeled [$^{203/212}$Pb]DOTA-conjugates elute from the HPLC column after the unlabeled peptide under reverse-phase gradient conditions. The developed separation procedure enhances the specific activity (radioactivity per amount of peptide that

is frequently used in PRRT, frequently reported in MBq $nmol^{-1}$ of peptide) to near theoretical levels (see Supplemental Information for calculation), which has the potential to prevent self-competition toward target receptors. In the *in vivo* pharmacokinetics study, we employed a B16F1 murine melanoma tumor model that is ideal for compound evaluation due to its high expression of MC1R target G-protein coupled receptor target. Results presented here corroborate the concept that [^{203}Pb]-labeled ligands can serve as surrogates to select patients and perform dosimetry in advance of [^{212}Pb]-labeled ligand therapy.

4.3. Automation of the methodology

The methodology for radiopharmaceutical production (including final separation/isolation of radiolabeled from unlabeled peptide) was adapted to an automated system for routine clinical radiopharmaceutical production to streamline processes and reduce radiation exposure to technical staff. This is especially important in the case of ^{212}Pb, which includes an intermediate daughter product ^{208}Tl that generates a highly energetic γ-ray (2.61 MeV). Therefore, ^{212}Pb radiolabeling must be conducted in a shielded environment (4–6″ Pb) or standard hot cell with manipulator arms and minimal close-hands-on effort is desired for production personnel.(Baidoo et al., 2013) The automated system was effective for production and isolation of Pb labeled final product compounds [$^{203/212}$Pb]DOTA-PEG4-VMT-MCR1. The complete automated production can be accomplished in approximately 1.5 h; and comprises all described procedural steps described for the hands-on methods described herein.

5. Conclusions

A refined radiolabeling method for [^{203}Pb/^{212}Pb]DOTA-conjugates that efficiently pre-concentrates and purify ^{203}Pb/^{212}Pb before radiolabeling has been adapted for automated production of ^{203}Pb/^{212}Pb radiopharmaceuticals for clinical applications. This method is suitable for wide range of chelator-modified-bioconjugates for radiolabeling and is suitable for routine production in clinical settings. Data presented corroborate with previous findings that [^{203}Pb]chelator-modified-bioconjugates are effective imaging surrogates in advance of [^{212}Pb] chelator-modified-bioconjugate therapy.

Supplementary Material

Refer to Web version on PubMed Central for supplementary material.

Acknowledgements

The authors thank and acknowledge the following University of Iowa organizations: the Free Radical and Radiation Biology Program, the Holden Comprehensive Cancer Center, the Central microscopy Research Facility, and the Flow Cytometry Facility. The authors kindly thank Professor Sue O'Dorisio for supplying DOTATOC for this study and Heather Henkins of the Missouri Research Reactor and the University of Missouri for helpful input on the manuscript. This work was partially supported by the following grants from the US National Institutes of Health: K25CA172218-01A1, 1P50CA174521-01A1, and 1-S10-RR025439-01.

References

Akabani G, Kennel SJ, Zalutsky MR, 2003 Microdosimetric analysis of alphaparticle-emitting targeted radiotherapeutics using histological images. J. Nucl. Med 44 (5), 792–805. [PubMed: 12732682]

Baidoo KE, Milenic DE, Brechbiel MW, 2013 Methodology for labeling proteins and peptides with lead-212 (^{212}Pb). Nucl. Med Biol 40 (5), 592–599. [PubMed: 23602604]

Bartlett M, 2016 From the inside out: radionuclide radiation therapy. Australas. Phys. Eng. Sci. Med 39 (2), 357–359. [PubMed: 27317024]

Behr TM, Behe M, Jungclas H, Jungclas H, Becker W, Sgouros G, 2001 Higher relative biological efficiency of alpha-particles: in vitro veritas, in vitro vanitas? Eur. J. Nucl. Med 28 (9), 1435–1436. [PubMed: 11585306]

Behr TM, Behe M, Stabin MG, Wehrmann E, Apostolidis C, Molinet R, Strutz F, Fayyazi A, Wieland E, Gratz S, Koch L, Goldenberg DM, Becker W, 1999 High-linear energy transfer (LET) alpha versus low-LET beta emitters in radioimmunotherapy of solid tumors: therapeutic efficacy and dose-limiting toxicity of ^{213}Bi-versus ^{90}Y-labeled CO17-1A Fab' fragments in a human colonic cancer model. Cancer Res 59 (11), 2635–2643. [PubMed: 10363986]

Elgqvist J, Frost S, Pouget JP, Albertsson P, 2014 The potential and hurdles of targeted alpha therapy - clinical trials and beyond. Front Oncol. 3, 324. [PubMed: 24459634]

Grieken RV, de Bruin M, 2009 Nomenclature for radioanalytical chemistry (IUPAC Recommendations 1994). Pure Appl. Chem. 66 (12), 2513–2526.

Hardiansyah D, Guo W, Kletting P, Mottaghy FM, Glatting G, 2016 Time-integrated activity coefficient estimation for radionuclide therapy using PET and a pharmacokinetic model: a simulation study on the effect of sampling schedule and noise. Med Phys. 43 (9), 5145. [PubMed: 27587044]

Hauck ML, Larsen RH, Welsh PC, Zalutsky MR, 1998 Cytotoxicity of alphaparticle-emitting astatine-211-labelled antibody in tumour spheroids: no effect of hyperthermia. Br. J. Cancer 77 (5), 753–759. [PubMed: 9514054]

Hobbs RF, Howell RW, Song H, Baechler S, Sgouros G, 2014 Redefining relative biological effectiveness in the context of the EQDX formalism: implications for alphaparticle emitter therapy. Radiat. Res 181 (1), 90–98. [PubMed: 24502376]

Horwitz EP, Chiarizia R, Dietz ML, 1992 A novel strontium-selective extraction chromatographic resin. Solvent Extr. Ion. Exch. 10 (2), 313–336.

Horwitz EP, Dietz ML, Rhoads Y, Felinto C, Gale NH, Houghton J, 1994 A lead-selective extraction chromatographic resin and its application to the isolation of lead from geological samples. Anal. Chim. Acta 292 (3), 263–273.

Humm JL, Chin LM, 1993 A model of cell inactivation by alpha-particle internal emitters. Radiat. Res 134 (2), 143–150. [PubMed: 8488249]

Iagaru AH, Mittra E, Colletti PM, Jadvar H, 2016 Bone-targeted imaging and radionuclide therapy in prostate cancer. J. Nucl. Med 57 (Suppl 3), 19S–24S. [PubMed: 27694165]

Jin ZH, Furukawa T, Degardin M, Sugyo A, Tsuji AB, Yamasaki T, Kawamura K, Fujibayashi Y, Zhang MR, Boturyn D, Dumy P, Saga T, 2016 alphaVbeta3 integrin-targeted radionuclide therapy with ^{64}Cu-cyclam-RAFT-c(-RGDfK-)4. Mol. Cancer Ther. 15 (9), 2076–2085. [PubMed: 27422811]

Jurcic JG, Larson SM, Sgouros G, McDevitt MR, Finn RD, Divgi CR, Ballangrud AM, Hamacher KA, Ma D, Humm JL, Brechbiel MW, Molinet R, Scheinberg DA, 2002 Targeted alpha particle immunotherapy for myeloid leukemia. Blood 100 (4), 1233–1239. [PubMed: 12149203]

Kim YS, Brechbiel MW, 2012 An overview of targeted alpha therapy. Tumour Biol. 33 (3), 573–590. [PubMed: 22143940]

Kratochwil C, Bruchertseifer F, Giesel FL, Weis M, Verburg FA, Mottaghy F, Kopka K, Apostolidis C, Haberkorn U, Morgenstern A, 2016a ^{225}Ac-PSMA-617 for PSMA targeting alpha-radiation therapy of patients with metastatic castration-resistant prostate cancer. J. Nucl. Med.

Kratochwil C, Giesel FL, Bruchertseifer F, Mier W, Apostolidis C, Boll R, Murphy K, Haberkorn U, Morgenstern A, 2014 ^{213}Bi-DOTATOC receptor-targeted alpha-radionuclide therapy induces remission in neuroendocrine tumours refractory to beta radiation: a first-in-human experience. Eur. J. Nucl. Med Mol. Imaging 41 (11), 2106–2119.

Kratochwil C, Giesel FL, Stefanova M, Benesova M, Bronzel M, Afshar-Oromieh A, Mier W, Eder M, Kopka K, Haberkorn U, 2016b PSMA-Targeted Radionuclide Therapy of Metastatic Castration-

Resistant Prostate Cancer with ^{177}Lu-Labeled PSMA-617. J. Nucl. Med 57 (8), 1170–1176. [PubMed: 26985056]

Kwekkeboom DJ, Krenning EP, 2016 Peptide receptor radionuclide therapy in the treatment of neuroendocrine tumors. Hematol. Oncol. Clin. North Am. 30 (1), 179–191. [PubMed: 26614376]

Li W, Liu Z, Li C, Li N, Fang L, Chang J, Tan J, 2016 Radionuclide therapy using (1)(3)(1)I-labeled anti-epidermal growth factor receptor-targeted nanoparticles suppresses cancer cell growth caused by EGFR overexpression. J. Cancer Res Clin. Oncol. 142 (3), 619–632. [PubMed: 26573511]

Lo Russo G, Pusceddu S, Prinzi N, Imbimbo M, Proto C, Signorelli D, Vitali M, Ganzinelli M, Maccauro M, Buzzoni R, Seregni E, de Braud F, Garassino MC, 2016 Peptide receptor radionuclide therapy: focus on bronchial neuroendocrine tumors. Tumour Biol.

Macklis RM, Kinsey BM, Kassis AI, Ferrara JL, Atcher RW, Hines JJ, Coleman CN, Adelstein SJ, Burakoff SJ, 1988 Radioimmunotherapy with alpha-particle-emitting immunoconjugates. Science 240 (4855), 1024–1026. [PubMed: 2897133]

Martin ME, O'Dorisio MS, Leverich WM, Kloepping KC, Walsh SA, Schultz MK, 2013 "Click"-cyclized (68)Ga-labeled peptides for molecular imaging and therapy: synthesis and preliminary in vitro and in vivo evaluation in a melanoma model system. Recent Results Cancer Res 194, 149–175. [PubMed: 22918759]

McDevitt MR, Sgouros G, Finn RD, Humm JL, Jurcic JG, Larson SM, Scheinberg DA, 1998 Radioimmunotherapy with alpha-emitting nuclides. Eur. J. Nucl. Med 25 (9), 1341–1351. [PubMed: 9724387]

Miao Y, Figueroa SD, Fisher DR, Moore HA, Testa RF, Hoffman TJ, Quinn TP, 2008 ^{203}Pb labeled alpha-melanocyte-stimulating hormone peptide as an imaging probe for melanoma detection. J. Nucl. Med 49 (5), 823–829. [PubMed: 18413404]

Miao Y, Hylarides M, Fisher DR, Shelton T, Moore H, Wester DW, Fritzberg AR, Winkelmann CT, Hoffman T, Quinn TP, 2005 Melanoma therapy via peptidetargeted {alpha}-radiation. Clin. Cancer Res 11 (15), 5616–5621. [PubMed: 16061880]

Miao Y, Quinn TP, 2008 Peptide-targeted radionuclide therapy for melanoma. Crit. Rev. Oncol. Hematol. 67 (3), 213–228. [PubMed: 18387816]

Nonnekens J, van Kranenburg M, Beerens CE, Suker M, Doukas M, van Eijck CH, de Jong M, van Gent DC, 2016 Potentiation of peptide receptor radionuclide therapy by the PARP inhibitor olaparib. Theranostics 6 (11), 1821–1832. [PubMed: 27570553]

Norain A, Dadachova E, 2016 Targeted radionuclide therapy of melanoma. Semin Nucl. Med 46 (3), 250–259. [PubMed: 27067506]

Otte A, 2016 Neuroendocrine tumors: peptide receptors radionuclide therapy (PRRT). Hell. J. Nucl. Med 19 (2), 182. [PubMed: 27331218]

Sgouros G, 2008 Alpha-particles for targeted therapy. Adv. Drug Deliv. Rev. 60 (12), 1402–1406. [PubMed: 18541332]

Sgouros G, Hobbs RF, Song H, 2011 Modelling and dosimetry for alpha-particle therapy. Curr. Radiopharm. 4 (3), 261–265. [PubMed: 22201712]

Sgouros G, Roeske JC, McDevitt MR, Palm S, Allen BJ, Fisher DR, Brill AB, Song H, Howell RW, Akabani G, Bolch WE, Brill AB, Fisher DR, Howell RW, Meredith RF, Sgouros G, Wessels BW, Zanzonico PB, 2010 MIRD Pamphlet No. 22 (abridged): radiobiology and dosimetry of alpha-particle emitters for targeted radionuclide therapy. J. Nucl. Med 51 (2), 311–328. [PubMed: 20080889]

Sgouros G, Song H, 2008 Cancer stem cell targeting using the alpha-particle emitter, ^{213}Bi: mathematical modeling and feasibility analysis. Cancer Biother Radiopharm. 23 (1), 74–81. [PubMed: 18298331]

Takahashi A, Miwa K, Sasaki M, Baba S, 2016 A Monte Carlo study on 223Ra imaging for unsealed radionuclide therapy. Med Phys. 43 (6), 2965. [PubMed: 27277045]

Wadas TJ, Pandya DN, Solingapuram Sai KK, Mintz A, 2014 Molecular targeted alpha-particle therapy for oncologic applications. AJR Am. J. Roentgenol. 203 (2), 253–260. [PubMed: 25055256]

Weber WA, Morris MJ, 2016 Molecular imaging and targeted radionuclide therapy of prostate cancer. J. Nucl. Med 57 (Suppl 3), 3S–5S.

Werner RA, Lapa C, Ilhan H, Higuchi T, Buck AK, Lehner S, Bartenstein P, Bengel F, Schatka I, Muegge DO, Papp L, Zsoter N, Grosse-Ophoff T, Essler M, Bundschuh RA, 2016 Survival prediction in patients undergoing radionuclide therapy based on intratumoral somatostatin-receptor heterogeneity. Oncotarget.

Wild D, Frischknecht M, Zhang H, Morgenstern A, Bruchertseifer F, Boisclair J, Provencher-Bolliger A, Reubi JC, Maecke HR, 2011 Alpha- versus beta-particle radiopeptide therapy in a human prostate cancer model (^{213}Bi-DOTA-PESIN and ^{213}Bi-AMBA versus ^{177}Lu-DOTA-PESIN). Cancer Res 71 (3), 1009–1018. [PubMed: 21245097]

Zalutsky MR, 2006 Targeted alpha-particle therapy of microscopic disease: providing a further rationale for clinical investigation. J. Nucl. Med 47 (8), 1238–1240. [PubMed: 16882999]

Zukotynski K, Jadvar H, Capala J, Fahey F, 2016 Targeted radionuclide therapy: practical applications and future prospects. Biomark. Cancer 8 (Suppl 2), 35–38. [PubMed: 27226737]

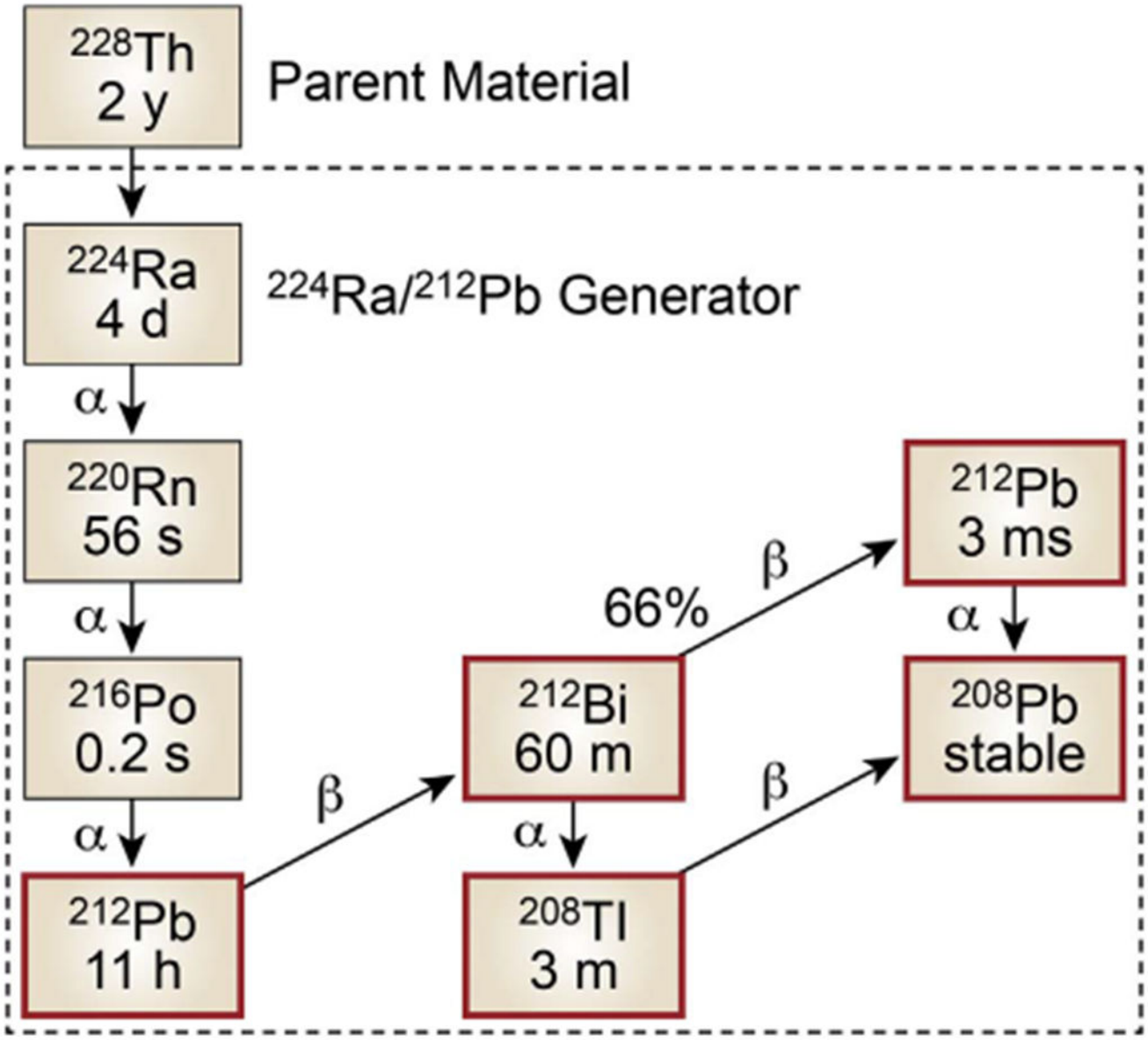

Fig. 1.

$^{224}Ra/^{212}Pb$ generator and decay scheme, including parent radionuclide ^{228}Th. ^{212}Pb is eluted periodically (approximately once every 24 h). The generator has a useful life that is governed by the 3.62 day half life of ^{224}Ra.

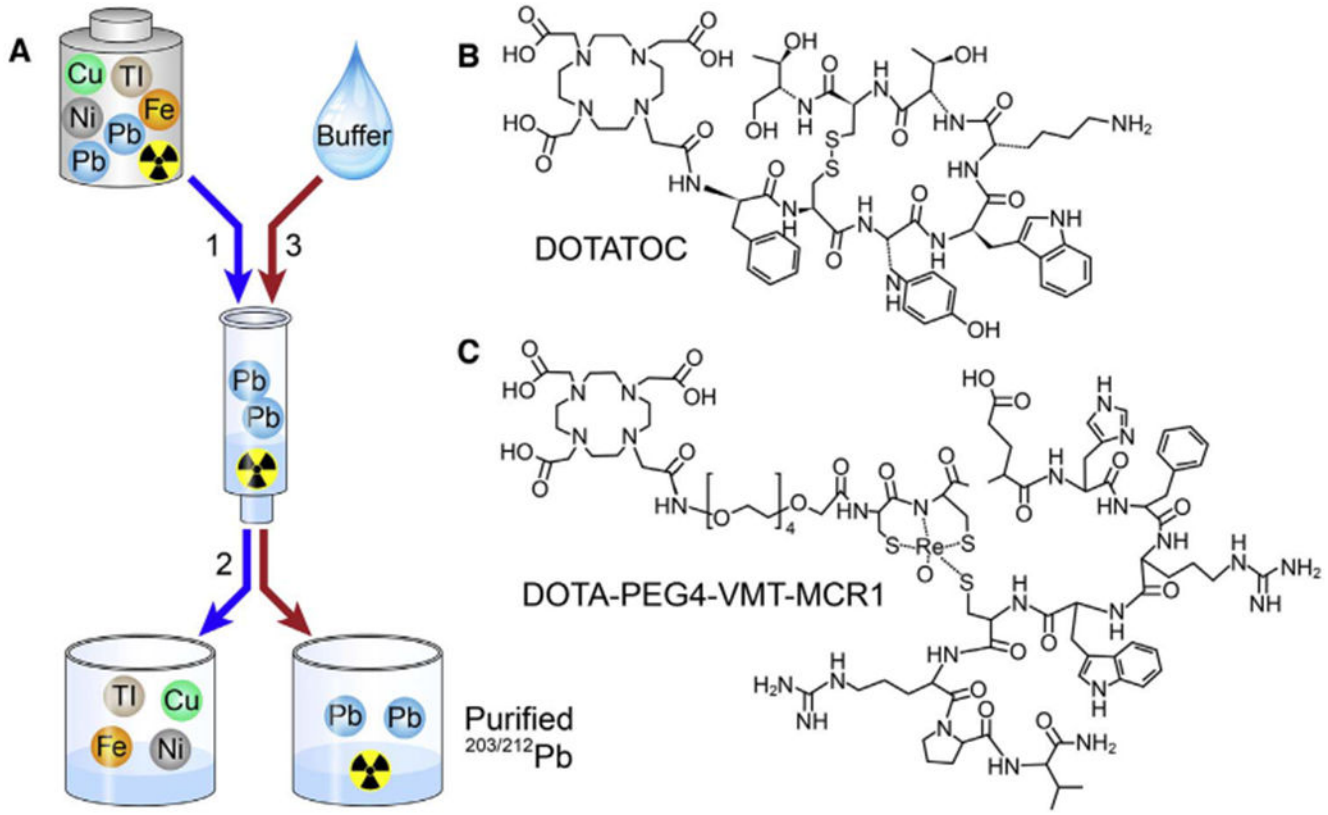

Fig. 2.

General workflow of $^{203/212}Pb$ pre-concentration and elution for radiolabeling of chelator-modified bioconjugates: (2-A1) Pre-concentration of $^{203/212}Pb^{2+}$ on the Pb-specific cartridge; (2-A2) Removal of metallic interferences with a HNO_3 rinse; (2-A3) Elution of the purified/pre-concentrated $^{203/212}Pb^{2+}$ by NaOAc buffer to the radiolabeling vessel containing chelator-modified bioconjugates; (B) Molecular structure of DOTATOC used for this study; (C) Molecular structure of DOTA-PEG4-VMT-MCR1 used for this study.

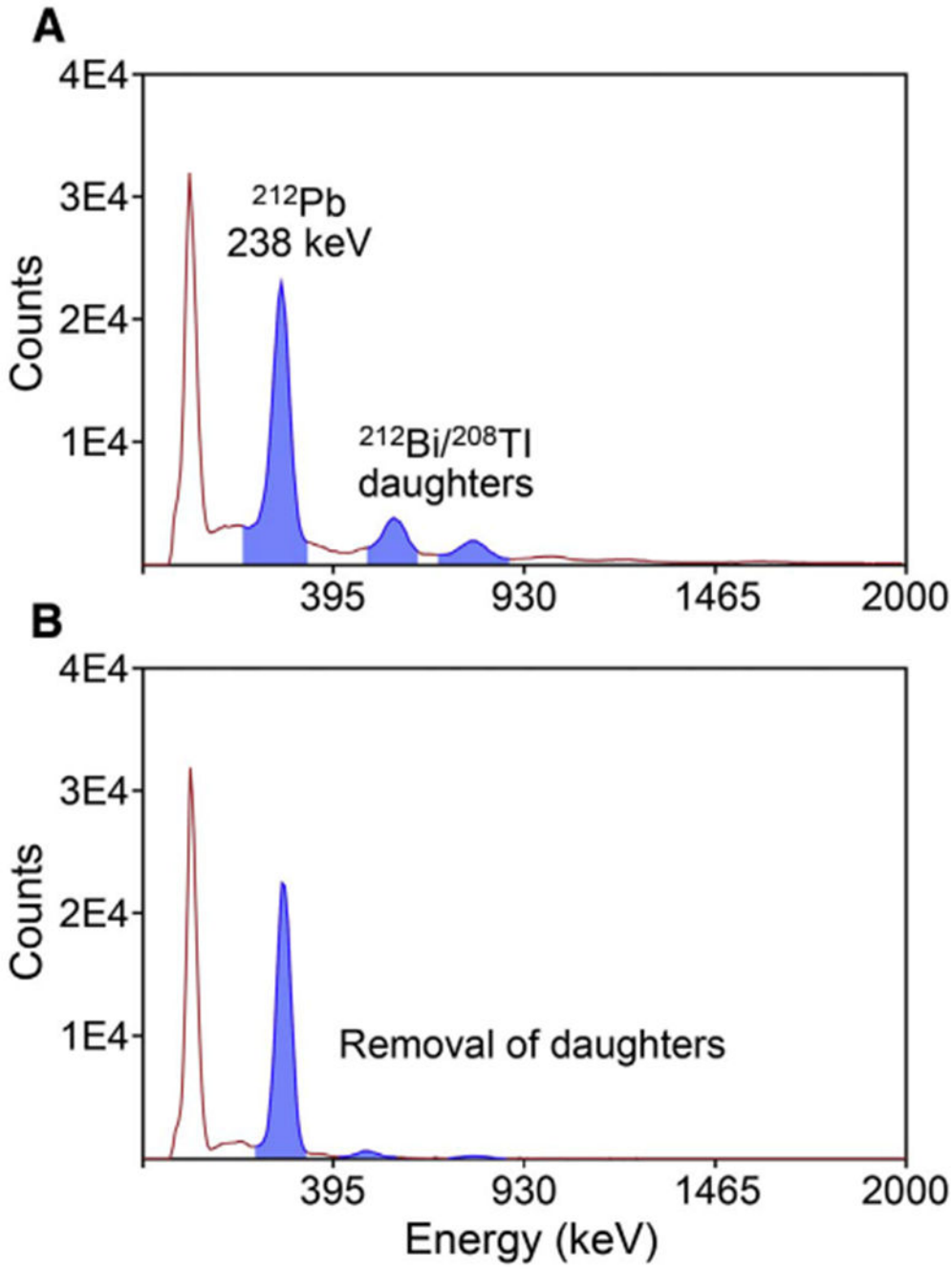

Fig. 3.

Gamma ray spectra of $^{224}Ra/^{212}Pb$ generator elution samples (A) before; and (B) after the Pb-resin pre-concentration/purification.

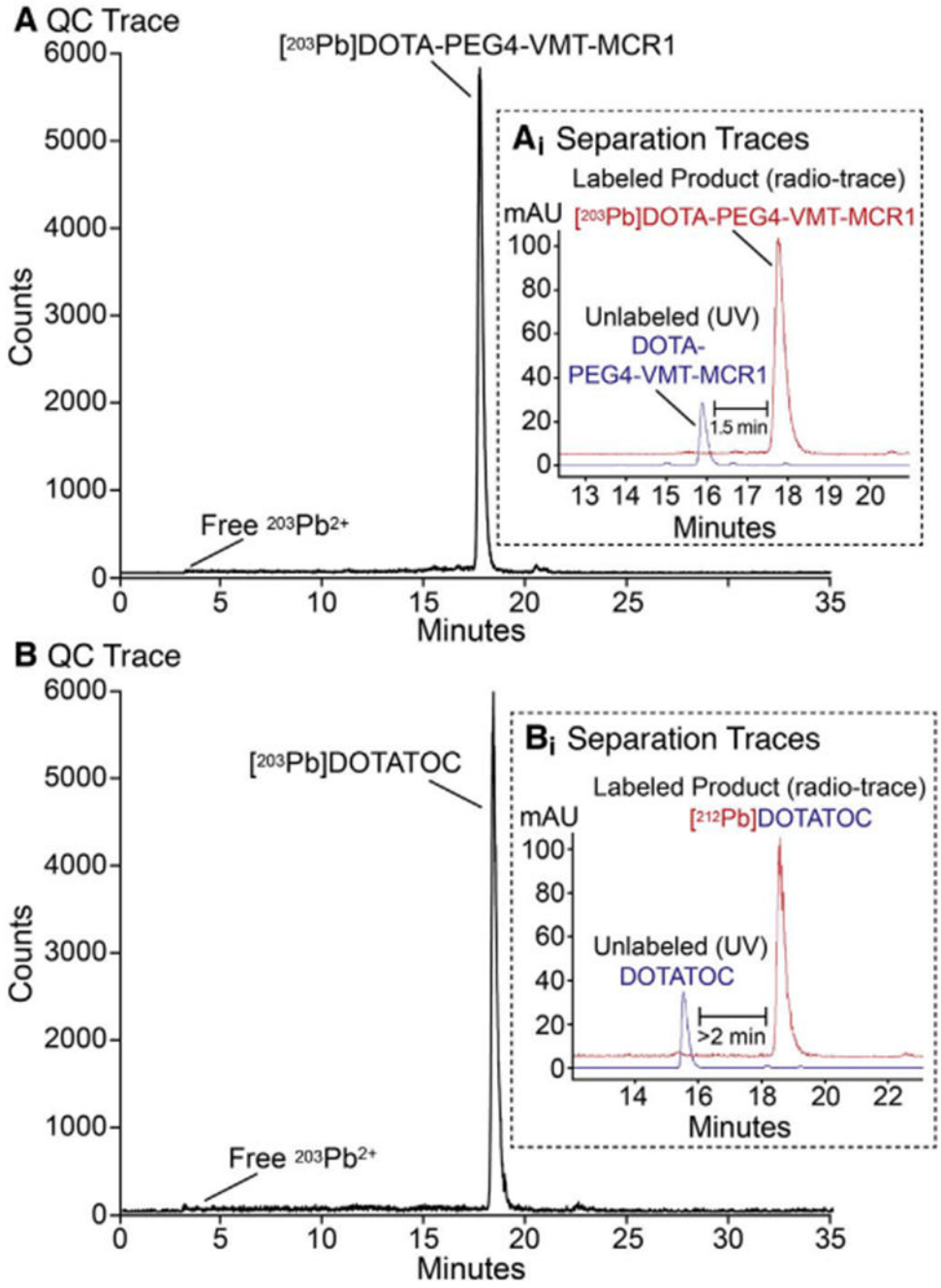

Fig. 4.

Determination of radiochemical purity of ^{203}Pb labeled peptides. (A) Radiochemical purity of [^{203}Pb]DOTA-PEG4-VMT-MCR1 by radio-HPLC tracing; and inset (A_i) HPLC isolation of labeled (in red) from unlabeled DOTA-PEG4-VMT-MCR1 precursor in blue (inset); (B) Radiochemical purity of [^{203}Pb]DOTATOC; and inset (B_i) isolation of labeled (in red) from unlabeled DOTATOC precursor in blue (inset).

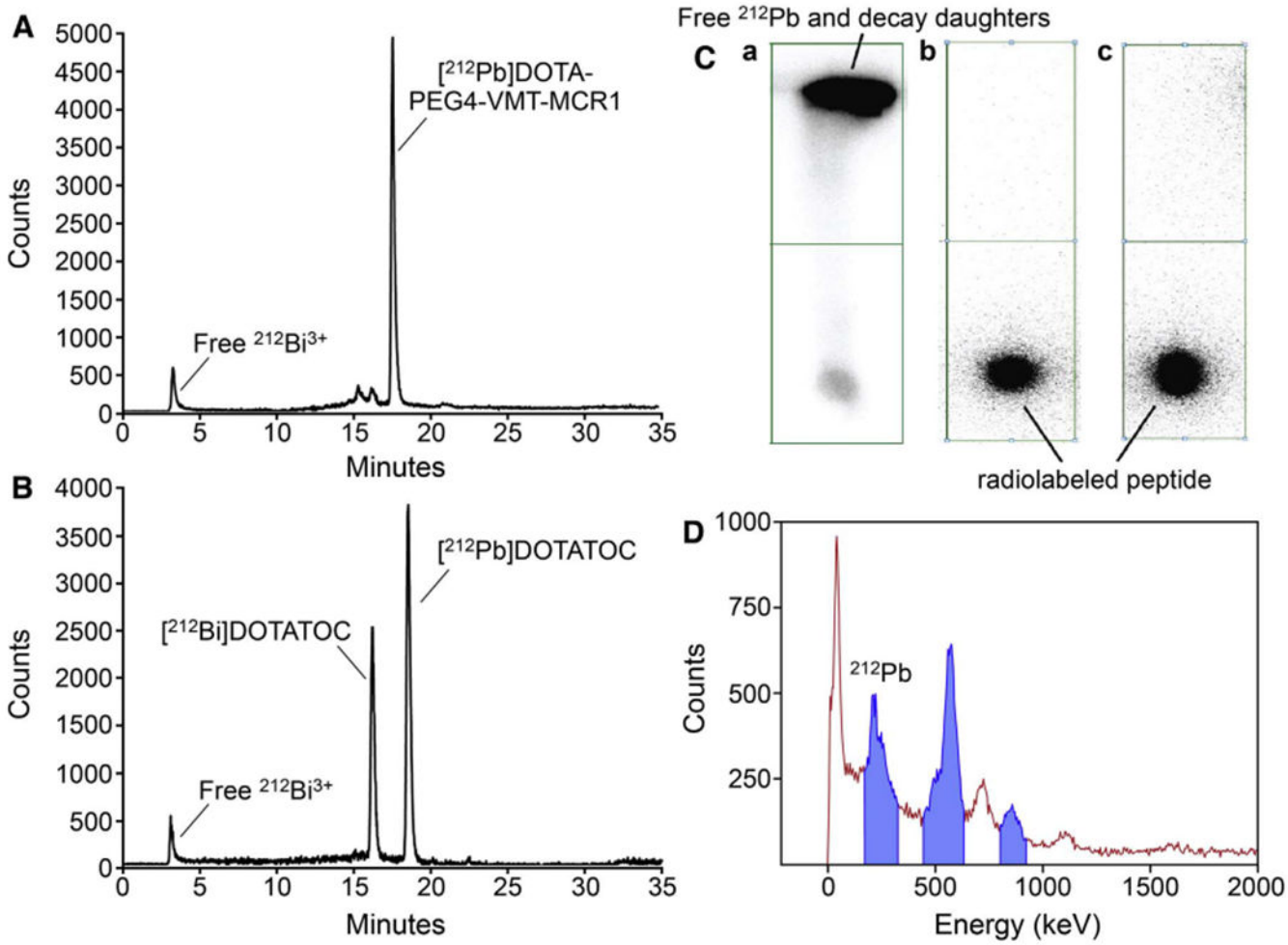

Fig. 5.

Determination of the radiochemical purity for ^{212}Pb labeled peptides. (A) Representative radio-HPLC chromatogram of [^{212}Pb]DOTA-PEG4-VMT-MCR1; (B) Representative radio-HPLC chromatogram [^{212}Pb]DOTATOC; (C_a) iTLC image showing solvent front migration of "free" (unlabeled) $^{212}Pb^{2+}$ and decay-product radionuclides; and (C_b) showing no migration of radioactivity with solvent front indicative of highly pure [^{212}Pb]DOTA-PEG4-VMT-MCR1; and (C_c) showing no migration of radioactivity with the solvent front; indicative of highly pure [^{212}Pb]DOTATOC; and (D) Representative gamma-ray energy spectrum of ^{212}Pb and ^{212}Bi from HPLC collection used to identify/quantify ^{212}Bi and ^{212}Pb.

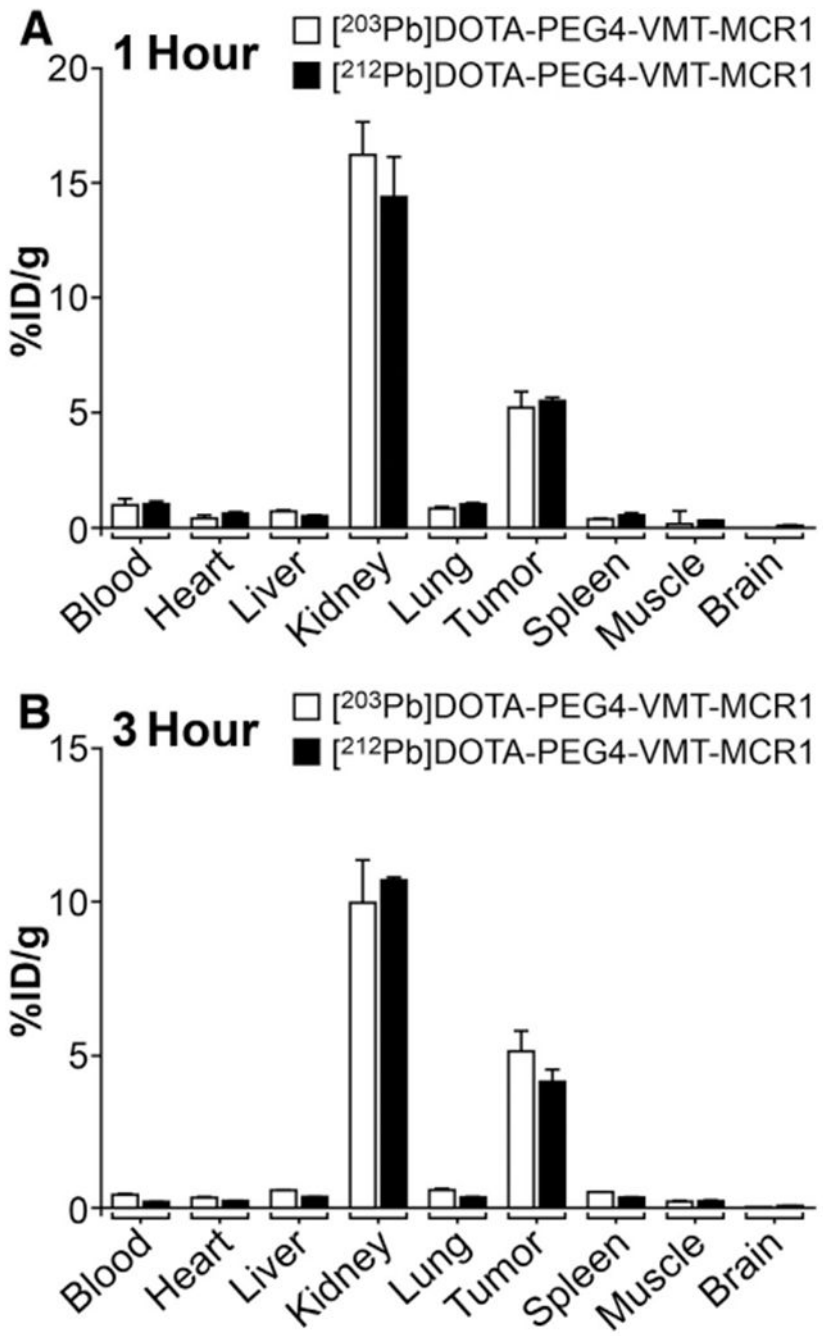

Fig. 6.

Comparison of the biodistribution of [^{203}Pb]DOTA-PEG4-VMT-MCR1 and [^{212}Pb] DOTA-PEG4-VMT-MCR1 in C57BL/6 mice bearing B16F1 murine melanoma tumor at (A) 1 h post tail vein injection; and (B) 3 h post tail vein injection. Data presented as percent injected dose per gram of tissue/blood (%ID/g; n =3 for each time point for each tissue ± SD). No significant difference in the biodistribution of [^{203}Pb]DOTA-PEG4-VMT-MCR1 and [^{212}Pb]DOTA-PEG4-VMT-MCR1 are observed.

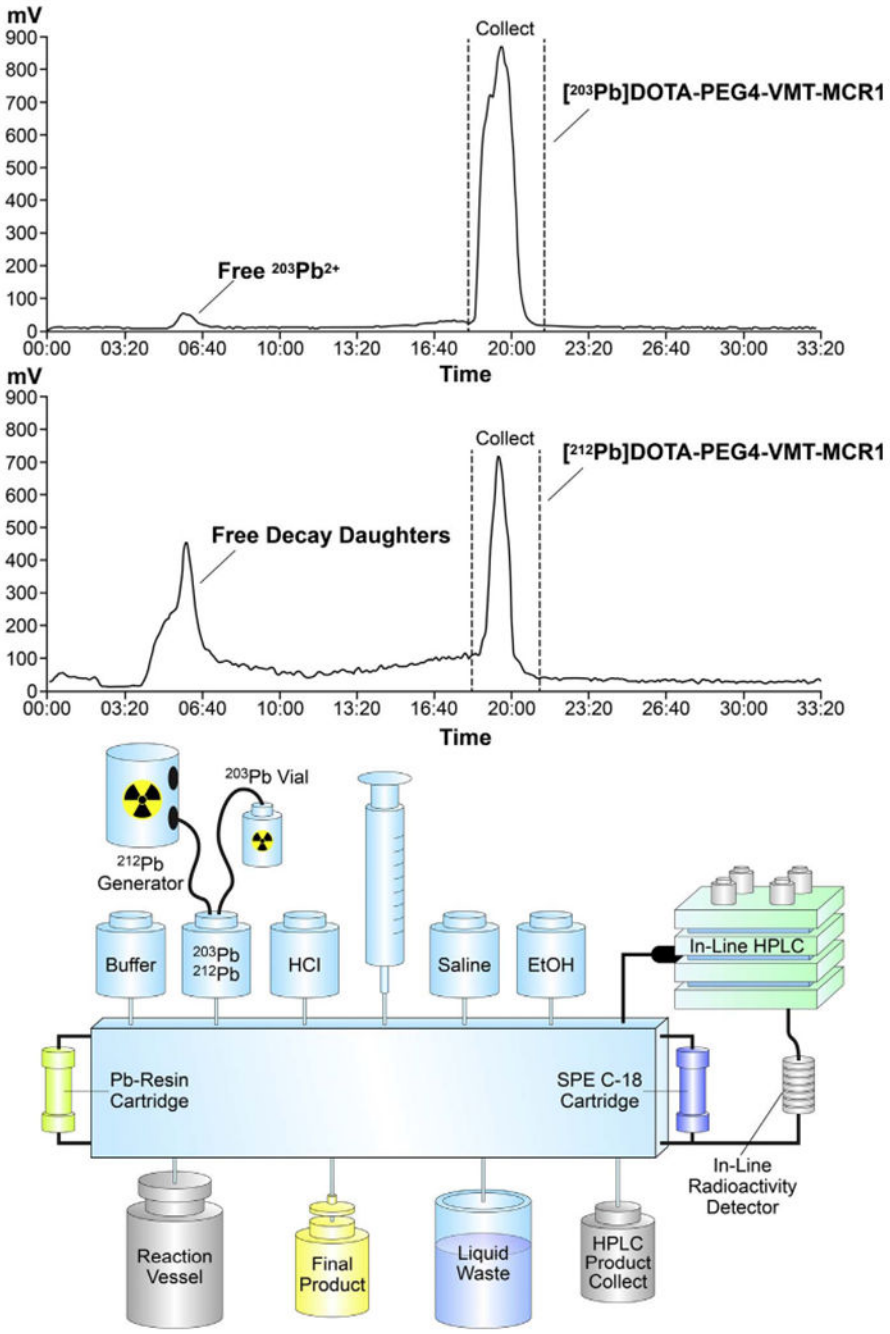

Fig. 7.

(A) Representative trace of radio-HPLC automated production and collection [$^{203/212}$Pb]DOTA-PEG4-VMT-MCR1 and (B) Scheme describing the Individual components of the Modular-Lab PharmTracer system adapted for production of [$^{203/212}$Pb]DOTA-PEG4-VMT-MCR1 radiopharmaceuticals (Eckert & Ziegler).

Table 1

Biodistribution of [^{203}Pb]DOTA-PEG4-VMT-MCR1 and [^{212}Pb]DOTA-PEG4-VMT-MCR1 in C57BL/6 mice bearing B16F1 murine melanoma tumors at 1 h and 3 h post tail vein injection. Data presented as percent injected dose per gram of tissue/blood (%ID/g; n = 3 for each time point for each tissue ± SD).

	1 h		3 h	
Tissue	**Pb-203**	**Pb-212**	**Pb-203**	**Pb-212**
	(%ID/g)	**(%ID/g)**	**(%ID/g)**	**(%ID/g)**
Blood	0.94 ± 0.30	1.05 ± 0.17	0.40 ± 0.02	0.17 ± 0.05
Heart	0.41 ± 0.13	0.62 ± 0.10	0.30 ± 0.07	0.19 ± 0.04
Liver	0.88 ± 0.08	0.49 ± 0.05	0.56 ± 0.03	0.35 ± 0.02
Kidneys	17.18 ± 1.30	14.76 ± 1.32	9.92 ± 1.44	10.65 ± 0.15
Lung	0.82 ± 0.38	1.00 ± 0.03	0.54 ± 0.08	0.33 ± 0.04
Tumor	5.20 ± 2.17	5.50 ± 0.23	5.27 ± 0.73	4.08 ± 0.46
Spleen	0.35 ± 0.18	0.52 ± 0.15	0.50 ± 0.04	0.31 ± 0.02
Muscle	0.14 ± 0.03	0.30 ± 0.03	0.18 ± 0.01	0.19 ± 0.07
Brain	0.04 ± 0.00	0.09 ± 0.02	0.06 ± 0.02	0.05 ± 0.01